Burns & Trauma, 2024, 12, tkae024
https://doi.org/10.1093/burnst/tkae024
Research Article

OXFORD

Research Article

Twist-related protein 1 promotes transforming growth factor β receptor 1 in keloid fibroblasts via regulating the stability of myocyte enhancer factor 2A

Tianhao Li[1], Mingzi Zhang[1], Yunzhu Li[1], Yixin Sun[1], Jiuzuo Huang[1], Ang Zeng[1], Nanze Yu[1,2,*] and Xiao Long[1,*]

[1]Department of Plastic and Aesthetic Surgery, Peking Union Medical College Hospital, Chinese Academy of Medical Sciences & Peking Union Medical College, 41 Damucang Hutong, Xicheng District, Beijing 100077, China and [2]Department of International Medical Service, Peking Union Medical College Hospital, Chinese Academy of Medical Sciences & Peking Union Medical College, 41 Damucang Hutong, Xicheng District, Beijing 100077, China

*Correspondence. Nanze Yu, Email: yunanze@pumch.cn; Xiao Long, Email: pumclongxiao@126.com

Received 20 November 2023; Revised 11 February 2024; Editorial decision 27 April 2024

Abstract

Background: Keloid scarring is caused by a fibroproliferative disorder due to abnormal activation of genes, the underlying mechanism of which is still unclear. The basic helix–loop–helix transcription factor Twist-related protein 1 (TWIST1) controls cell proliferation and differentiation in tissue development and disease processes. In this study, we aimed to clarify the essential role of TWIST1 in the pathogenesis of keloids.

Methods: Immunohistochemistry, cell counting kit-8 assays, western blotting, PCR, matrigel invasion assays and immunofluorescence assays were applied to demonstrate the effects and mechanisms of TWIST1 in fibroblasts derived from normal skin and keloids. Mass spectrometry, ubiquitination assays, chromatin immunoprecipitation and dual luciferase reporter assay were applied to explore the interaction of TWIST1 with downstream molecules.

Results: In the present study, we confirmed that TWIST1 was upregulated in keloid tissue of patients and in keloid-derived fibroblasts (KFBs). *In vitro*, TWIST1 inhibition prevented KFB proliferation, invasion and activation. We also discovered a link between TWIST1 and the transforming growth factor β (TGF-β) signaling related molecules TGF-β receptor 1 (TBR1), SMAD family member 2 (Smad2) and Smad3, and the fibrosis markers α-smooth muscle actin, collagen type I and collagen type III in KFBs. Mechanistically, we uncovered a brand-new mechanism by which TWIST1 interacts with myocyte enhancer factor 2A (MEF2A) and suppresses its ubiquitination and degradation. Using chromatin immunoprecipitation and dual-luciferase reporter assay, TBR1 was identified as a novel downstream target of MEF2A, which directly binds to its promoter. Overexpression of TWIST1 promoted the recruitment of MEF2A to the TBR1 promoter and restored TBR1 functional expression.

Conclusions: Our research highlights a significant function of TWIST1 in the development of keloid and its related fibroblasts, partially facilitated by elevated MEF2A-dependent TBR1 expression. Blocking the expression of TWIST1 in KFBs could potentially pave a novel therapeutic avenue for keloid treatment.

Key words: Ubiquitination, Keloid-derived fibroblasts, Twist-related protein 1, Myocyte enhancer factor 2A, Transforming growth factor β receptor 1, Transcription factor

Highlights

- TWIST1 is upregulated in keloid tissue and keloid-derived fibroblasts.
- TWIST1 affects the proliferation and invasion of keloid-derived fibroblasts and the expression of TGFβ/Smad signaling.
- TWIST1 interacts with MEF2A and suppresses its ubiquitination and degradation.
- TBR1 is a direct target of MEF2A in keloid-derived fibroblasts.

Background

With a 4.5–16% incidence rate, keloid is a fibroproliferative skin disease that is typically caused by burn injuries, trauma and contagious skin diseases. It is most frequently observed in sub-Saharan Africans, African Americans and Asians [1–3]. Therapeutically, keloids seldom subside, frequently outgrow the boundaries of the initial wound, invade nearby normal tissues and typically exhibit a tumor tendency [4]. To date, no effective intervention has been able to overcome the post-treatment reoccurrence of keloids. Invading keloid scars put patients under a great deal of psychological stress in addition to their unaesthetic appearance and regional aggravating symptoms [5–7]. Evidently, more research is still needed to better understand keloid pathophysiology and determine viable treatments.

One of the aberrant behaviors of keloids is continuous invasion into the surrounding tissue. Moreover, fibroblasts are critical in the etiology of keloid lesions due to their active participation in collagen formation [8,9]. While having a comparable shape to normal skin-derived fibroblasts (NFBs), keloid-derived fibroblasts (KFBs) exhibit tumor-like characteristics, including a high ability to proliferate and invade and accelerated release of extracellular matrix (ECM) [10–13]. We thus postulate that decreasing the activity of KFBs and lowering their collagen synthesis would be highly significant against invading keloids.

Twist-related protein 1 (TWIST1), a transcription factor belonging to the basic helix–loop–helix family, is a key regulator of cellular homeostasis but also has a role in the genesis of diseases, including carcinoma [14]. TWIST proteins are crucial for mesenchymal differentiation during embryonic development [15]. TWIST1 can facilitate epithelial-to-mesenchymal transition (EMT) after injury and control mesenchymal tissue responses in adults [16,17]. Nevertheless, abnormal TWIST1 expression could result in pathological EMT and support the development of neoplasia and tissue fibrosis [18,19]. Transforming growth factor (TGF)/SMAD family member 3 (SMAD3)/p38 are needed for TWIST1 to behave as a profibrotic factor [20,21]. In previous research, we applied single-cell sequencing and bulk RNA-sequencing to demonstrate that keloid fibroblasts express TWIST1 excessively [10]. The impact of TWIST1 on keloids and the underlying processes, however, are yet unclear. Furthermore, strong evidence suggests that the TGF signaling pathway is crucial for the development of keloids and other fibrotic diseases [22]. The TGFβ1 ligand has the ability to convert fibroblasts into myofibroblasts, which produce significant amounts of collagen fibers, a characteristic of keloids [23,24]. Additionally, TGF signaling has also been linked to tumor angiogenesis [22].

In the present study, we confirmed the expression of TWIST1 in the keloid tissue of patients and in KFBs. We also investigated the correlation between TWIST1 and the TGF-β signaling pathway in KFBs. In addition, we uncovered a novel mechanism by which TWIST1 enhances the proteasomal degradation of myocyte enhancer factor 2A (MEF2A), a recently discovered transcription factor for TGF-β receptor 1 (TBR1) expression. We also discovered how this mechanism underlies how TWIST1 promotes KFB proliferation and invasion. According to the study's findings, TWIST1 may be a useful therapeutic target for treating keloid and other fibroproliferative illnesses.

Methods

Specimen collection

Ten normal skin tissues and keloid scar tissues to be used for plastic surgery were obtained from Peking Union Medical College Hospital after receiving ethical permission from the hospital's local human study Ethics Council in line with the Declaration of Helsinki's tenets. Using keloid scar tissues and normal skin tissues, primary human KFBs and NFBs were extracted. Information on the patients is provided in Table S1, see online supplementary material. Written consent was obtained from the patients.

Histology and immunohistochemistry

Tissues were embedded in paraffin, fixed overnight in paraformaldehyde and then dissected. Hematoxylin and eosin or Masson's trichrome was used to stain the slices. Sections were stained using an anti-TWIST1 primary antibody (CST, 69366, 1 : 300) and anti-MEF2A primary antibody (Santa Cruz, sc-17 785, 1 : 300) for immunohistochemistry at 4°C overnight. The following day, the sections were counterstained with hematoxylin and developed using diaminobenzidine after being treated with an Horseradish Peroxidase (HRP)-conjugated secondary antibody overnight. Image-Pro Plus 6.0 software was utilized for quantitative analysis.

Cell isolation and culture

Human KFB and NFB isolation steps were as described in our previous study [10]. Following excision, the scar sample was washed three times in sterile 1x phosphate buffer solution (PBS) before being immersed in a 0.25% trypsin solution and stored at 4°C overnight. The next day, the epidermis was removed and the scar was trimmed. Then, digestion with 0.25% collagenase IV solution was performed for 4 h at 37°C; 200-mesh sieving is needed. Centrifuging was carried out at 1000 rpm for 5 min. The cells were maintained in Dulbecco's modified Eagle's medium (HyClone) supplemented with 10% fetal bovine serum (FBS) (Sigma–Aldrich) and 1% penicillin/streptomycin antibiotics (HyClone). The medium was replaced every 2 to 3 days and observed with a contrast microscope. Once the fusion occupies about 80% of the bottom area of the Petri dish, passage is possible [25]. Subsequent experiments used four to seven generations of cells. TGF-β1 was applied to cells in certain groups at concentrations of 5 and 10 ng/ml (HZbscience).

Transfection and grouping of fibroblasts

Each well of a 6-well plate contained 3×10^5 cells. The following day, transfection of small interfering (si)RNA or plasmids was carried out in accordance with the recommended procedures using Lipofectamine 3000 (Thermo Scientific). For the purpose of creating stable TWIST1-overexpressing cell cultures, lentiviral transduction was carried out. A multiplicity of infection of 10 was used to infect 2×10^5 cells with TWIST1-overexpression lentiviruses from Shanghai Genechem. The cells were grown in medium with 2 mg/l puromycin for 2 weeks after being infected for 72 h to eliminate noninfected cells. Information about the siRNA sequence is provided in Table S2, see online supplementary material.

Quantitative real-time PCR

Following the manufacturer's instructions, total RNA from the cells was extracted using TRIzol reagent (Thermo Fisher Scientific). Reverse transcription of the RNA was then carried out using the RevertAid First Strand cDNA Synthesis Kit (Thermo Fisher Scientific). Quantitative real-time PCR was carried out using PowerUp SYBR Green Master Mix (Thermo Scientific). The internal reference gene β-actin was used, and fold enrichment was verified by computing the $\Delta\Delta$Ct value. The primers used in this study are presented in Table S3, see online supplementary material.

Western blot analysis

To extract proteins from cells, RIPA lysis buffer (P0013B, Beyotime, China) was utilized. The protein concentration was determined using the BCA Protein Assay Kit (P0012, Beyotime, China). Before Western blotting, the protein lysates from each cell were combined with sodium dodecyl sulfate (SDS) buffer and boiled at 100°C for 10 min. For each well, the total amount of protein sampled was estimated to be 20 μg. The proteins were electrophoretically separated in an SDS–polyacrylamide gel and then transferred to a PVDF membrane. After that, the PVDF membrane was blocked for 90 min with 5% milk in tris-buffered saline with 0.05% Tween (TBST).

The membranes were then exposed to primary antibodies at 4°C for an overnight incubation. Following a second TBST wash, the membranes were incubated for 60 min with a second antibody before being thoroughly cleaned with TBST. A chemiluminescence detection kit (P0018S, Beyotime, China) and an automated chemiluminescence image processing system were then utilized to observe the proteins on the PVDF membrane (Tanon, China). ImageJ software was used to further quantify the protein bands. The primers utilized in this study are presented in Table S4, see online supplementary material.

Immunofluorescence

Protein expression was observed using an immunofluorescence assay. The primary antibody was anti-α-SMA (14395–1-AP, Proteintech). As the secondary antibody, Alexa Fluor 488 (A0423, Beyotime) was utilized. Transfected cells ((2×10^4) were implanted in each chamber of an eight-chambered cover glass (Corning, USA). After cell adhesion, the cells were treated for 15 min with 4% paraformaldehyde to fix them. A 3% BSA solution at 37°C was employed to seal off for 30 min. The cells were then incubated with the primary antibody overnight at 4°C and with the secondary antibody for 50 min at 37°C. The nuclei were finally stained using 2-(4-Amidinophenyl)-6-indolecarbamidine dihydrochloride (DAPI) (C1006, Beyotime). A laser confocal microscope was used to visualize and capture immunofluorescence (Nikon).

Cell counting kit-8 assay

The cell counting kit-8 (CCK-8) assay kit (Dojindo Laboratories) was used to evaluate the rate of cell proliferation. In brief, 96-well plates were first seeded with KFBs at 5000 cells per well. On the first day following transfection, the transfected cells were plated. At 0, 24, 48, 72 and 96 h after seeding, 10 μl of the CCK-8 reagent was applied to each well. After 2 h, all plates were scanned by a microplate reader (Thermo Fisher Scientific). Four replicates were used in the experiment. Measurements of absorbance at 450 nm were used to assess cell proliferation.

Matrigel invasion assays

The ability of KFBs to invade was assessed using 8-mm membrane pore transwell chambers (Corning) that were precoated with Matrigel (BD Biosciences). A 60 μl volume of dilute Matrigel gel, 1 : 9 with serum-free cell culture medium, at 4°C was added to each chamber and incubated for 3 h at 37°C. The bottom chambers were then filled with 500 ml of 10% FBS containing Dulbecco's modified Eagle's medium. The top chambers were seeded with 5000 cells per well in serum-free medium. As the cultures were prepared for the

invasion test, we removed the top chambers and any adherent cells in a half-circle on either the upper or bottom side of the membranes. The adhering cells were then treated with methanol and stained with 0.5% crystal violet (Olympus, Japan) and cell counting was performed using an optical microscope in three randomly selected regions of each side of the membrane.

Co-immunoprecipitation Using a specific lysis buffer for immunoprecipitation, human KFB proteins were obtained. Thermo Fisher Scientific's BCA kit was used to assess the protein concentrations in the lysates after centrifugation, and the lysates were then softly rocked at 4°C overnight. Lysates were treated with protein A/G-agarose (Thermo Fisher Scientific) prebound to anti-TWIST1 or anti-MEF2A antibody for 2 h to perform immunoprecipitation. A total of 400 μg of total protein was utilized with ~3 μl of antibodies. Precipitated proteins were boiled in 2× sample loading buffer and then separated by 15 or 12% SDS–PAGE after being washed five times with cell lysis solution. The separated protein was transferred to a PVDF membrane and immunoblotted using an anti-TWIST1 or anti-MEF2A antibody, as appropriate. Immunoglobulin G (IgG) served as the negative control.

Mass spectrometry

The proteins in the elution were precipitated by adding four volumes of cold acetone after an overnight immunoprecipitation at 4°C. Protein samples were dissolved in 8 mol/l urea/100 mmol/l Tris–HCl after drying in air (pH 8.0). After being reduced with 10 mmol/l Dithiothreitol (DTT) at 37°C for 60 min, cysteine was alkylated in the dark with 40 mmol/l iodoacetamide at ambient temperature for 30 min. Urea was diluted to <2 mol/l (pH 8.0) with 100 mmol/l Tris–HCl. After desalting the peptides using StageTip C18 and vacuum drying them, trypsin was added for overnight digestion at 37°C. The resultant tryptic peptides were examined using a TripleTOF 5600 LC–MS/MS mass spectrometry (MS) system. The peptides were initially put onto an Agilent Technologies C18 trap column (5 μm, 5 × 0.3 mm) and then eluted into an Eksigent C18 analytical column (75 μm × 150 mm, 3 μm particle size, 100 pore size). Dimethyl sulfoxide (DMSO) (3%), 97% H_2O and 0.1% formic acid were used in mobile phase A, while 3% DMSO, 97% ACN and 0.1% formic acid were used in mobile phase B to create a 100-min separation gradient. A constant flow rate of 300 nl/min was used. Each scan cycle for information-dependent acquisition (IDA) mode analysis included 40 MS/MS events (m/z ranging from 100 to 1500, ion accumulation period 50 ms) after full-scan mass spectra (m/z ranging from 350 to 1500, ion accumulation time 250 ms) were obtained. For +2 to +5 precursors, the MS/MS acquisition activation threshold was set at 120 cps. The previous target-ion exclusion time was 18 s. ProteinPilot (V4.5) searches were made using the Paragon algorithm against the proteome reference database for humans in UniProt. Unused ≥1.3 was utilized to filter search results, database entries and tainted proteins were removed, and the identification data that remained were used for further research.

Ubiquitination assays

KFBs were maintained in a 25 × 25 cell container and given a further 12 h of proteasome inhibitor treatment with MG132 (10 mol/l). Total cell lysates were created using 20 mmol/l Tris–HCl, pH 7.5, 150 mmol/l NaCl, 10 mmol/l EDTA, 1% Triton X-100, 1% deoxycholate and a protease inhibitor cocktail as the lysis buffer (Roche). Sonication and centrifugation were used to lyse the cells. The supernatants were then collected, treated with an anti-MEF2A antibody overnight at 4°C and then incubated with protein A/G-agarose for 2 h. Centrifuging, collecting, washing, suspending and using antibodies against ubiquitin or MEF2A were conducted prior to western blot examination of the immunoprecipitates.

Chromatin immunoprecipitation

KFBs were harvested, fixed with 1% formaldehyde in PBS for 10 min and washed with ice-cold PBS. Cells were subsequently sonicated to generate DNA fragments, which were immunoprecipitated with anti-MEF2A or control IgG (26 157, Thermo Scientific). Immunoprecipitated chromatin fragments were quantified by real-time PCR and normalized against total input genomic DNA. Primer sequences were designed to span the predicted consensus elements of the MEF2A binding motif within the TBR1 promoter by use of the freeware Jaspar (http://jaspar.genereg.net/). The primers utilized in this study are presented in Table S5, see online supplementary material.

Dual-luciferase reporter assay

To determine whether the gene promoter was activated, a dual-luciferase reporter study was performed. For the dual-luciferase reporter test, the control lentivirus-CON254 and lentivirus-TWIST1 cell lines were created. Cells were transfected with either the wild-type or mutant human TWIST1-promoter-luciferase reporter and seeded in 6-well plates. Following a 48-h transfection, the cells were lysed and a dual-luciferase reporter assay was conducted as directed by the Dual Luciferase Reporter Gene Assay Kit (Yeasen Biotechnology). A multipurpose microplate reader was used to measure the bioluminescence.

Statistical analysis

The information is shown as the means and standard deviation. Comparison between the means of two groups of scar tissue and normal skin tissue of the same patient is performed by the paired samples t-test. Two factor repeated measures of variance was applied to analysis the difference. If three or more groups were compared, analysis of variance was followed by Tukey's post hoc test. Statistics were judged significant at $p < 0.05$. Each experiment was run at least three times. The Prism 8 program was used to create the graphs and pictures.

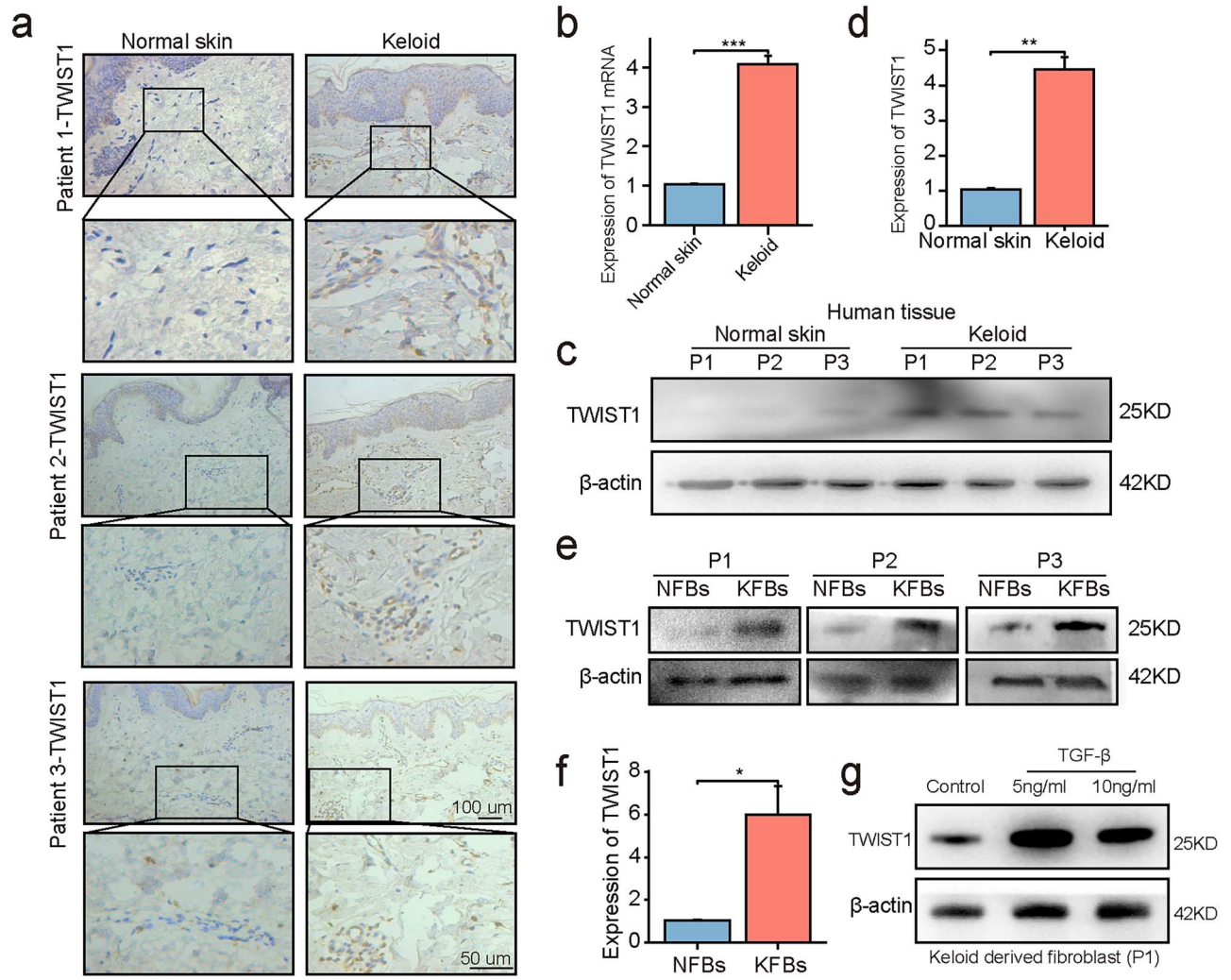

Figure 1. TWIST1 is upregulated in keloid tissue and keloid-derived fibroblasts. (**a**) The expression levels of TWIST1 were detected in keloid and paired normal tissue by immunohistochemistry (Scale bar: 100 μm & 50 μm). (**b**) mRNA expression level of TWIST1 was measured in keloid and normal skin tissue by real-time PCR. (**c**, **d**) Western blotting was used to measure the protein expression level of TWIST1 keloid tissues and paired normal skin tissues with densitometry analysis of western blot results. (**e**, **f**) Western blot results of TWIST1 in keloid-derived fibroblasts and normal skin-derived fibroblasts. (**g**) Western blot results of TWIST1 in keloid-derived fibroblasts with 0, 5 and 10 ng/ml TGF-β1. $^{*}p < 0.05$, $^{**}p < 0.01$, $^{***}p < 0.001$. *NFBs* normal skin-derived fibroblasts, *KFBs* keloid-derived fibroblasts, *TWIST1* Twist-related protein 1, *TGF-β* transforming growth factor beta

Results

Expression of TWIST1 is increased in keloid tissues

Hematoxylin and eosin staining revealed that the dermis of keloid tissues contained more fibroblasts and disordered collagen fibrils than comparable normal skin tissues. In contrast to matching normal skin tissues, Masson staining showed that the location of collagen fibrils in keloid tissues was chaotic, and that the quantity of collagen was higher (Figure S1, see online supplementary material).

The levels of TWIST1 mRNA and protein expression in keloid and normal skin tissues and cell lines were obtained using RT–PCR, western blotting and immunohistochemistry. TWIST1 protein expression was markedly higher in keloid skin tissue than in matching normal skin tissue, according to the RT–PCR, western blotting and immunohistochemistry results (Figure 1a–d; $p < 0.01$). According to the western blot results, TWIST1 was upregulated in KFBs compared to NFBs (Figure 1e, f). TWIST1 protein concentrations considerably increased after 24 h of incubation with TGF-β1 at concentrations of 5 and and 10 ng/ml (Figure 1g).

TWIST1 facilitates KFB proliferation and invasion

RT–PCR and western blotting were used to confirm the transfection effectiveness. Based on knockdown efficiency, we chose si-TWIST1–001 for the next step of research. As expected, the mRNA and protein expression levels were dramatically downregulated in the group treated with small interfering RNA TWIST1–001 compared to the small interfering negative control groups (Figure S2a, b, see online supplementary material). In contrast, the TWIST1 group exhibited greatly upregulated mRNA and protein

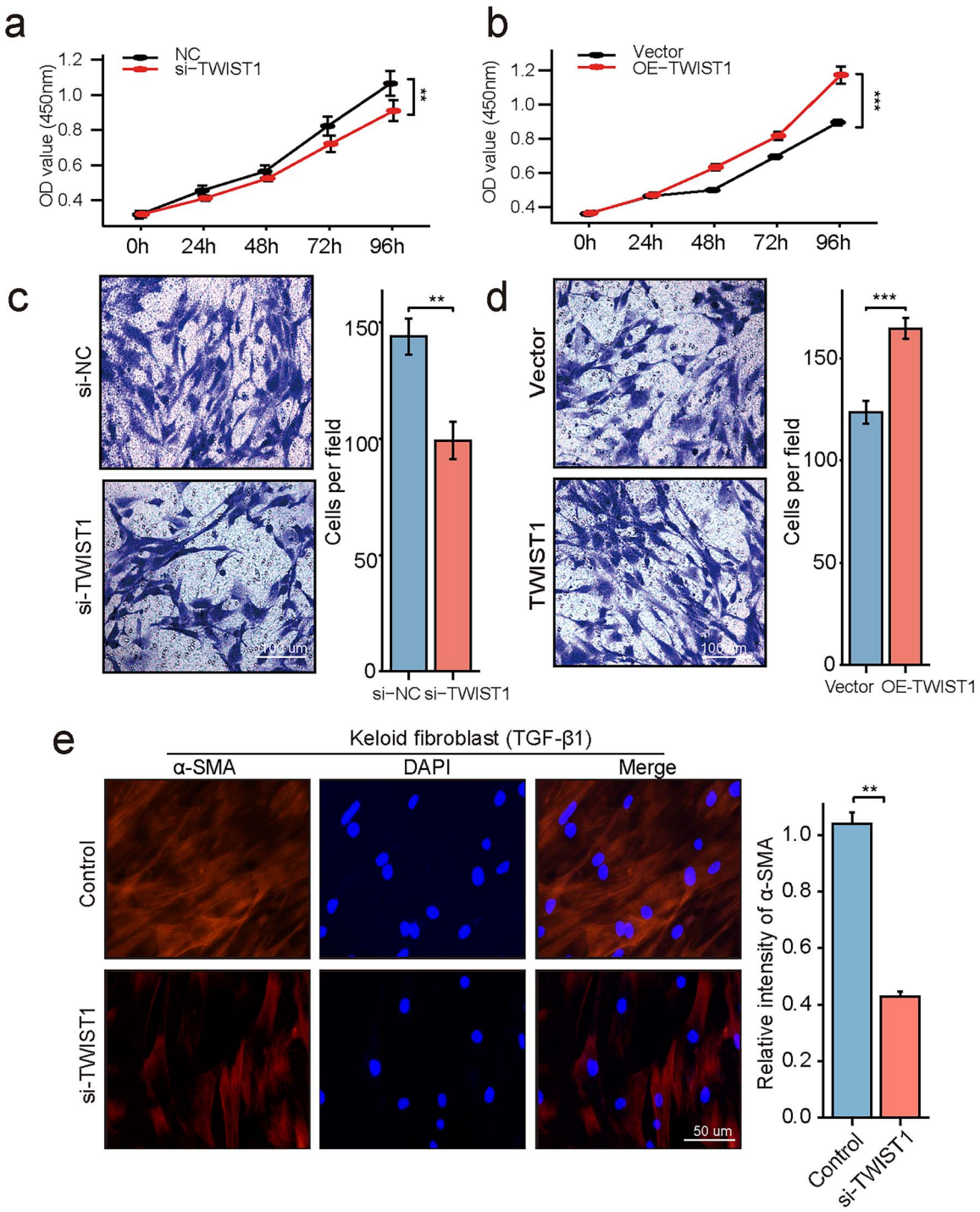

Figure 2. Knockdown and overexpression of TWIST1 affect the proliferation and invasion of keloid-derived fibroblasts. (**a**) Proliferation of keloid-derived fibroblasts in small interfering negative control and small interfering TWIST1 groups was detected by the cell counting kit-8 assay. (**b**) Proliferation of keloid-derived fibroblasts in vector and TWIST1 groups was detected by cell counting kit-8 assay. (**c**) Invasion ability of keloid-derived fibroblasts in small interfering negative control and small interfering TWIST1 groups was detected by transwell assays (Scale bar: 100 μm). (**d**) Invasion of keloid-derived fibroblasts in vector and TWIST1 groups was detected by transwell assays (Scale bar: 100 μm). (**e**) Immunofluorescence assay of α-SMA in keloid-derived fibroblasts with 5 ng/ml TGF-β1 (Scale bar: 50 μm). $^{**}p < 0.01$, $^{***}p < 0.001$. *TWIST1* Twist-related protein 1, *TGFβ1* transforming growth factor 1, *si* small interfering, *OD* optical density, *OE* over-expression, *NC* negative control

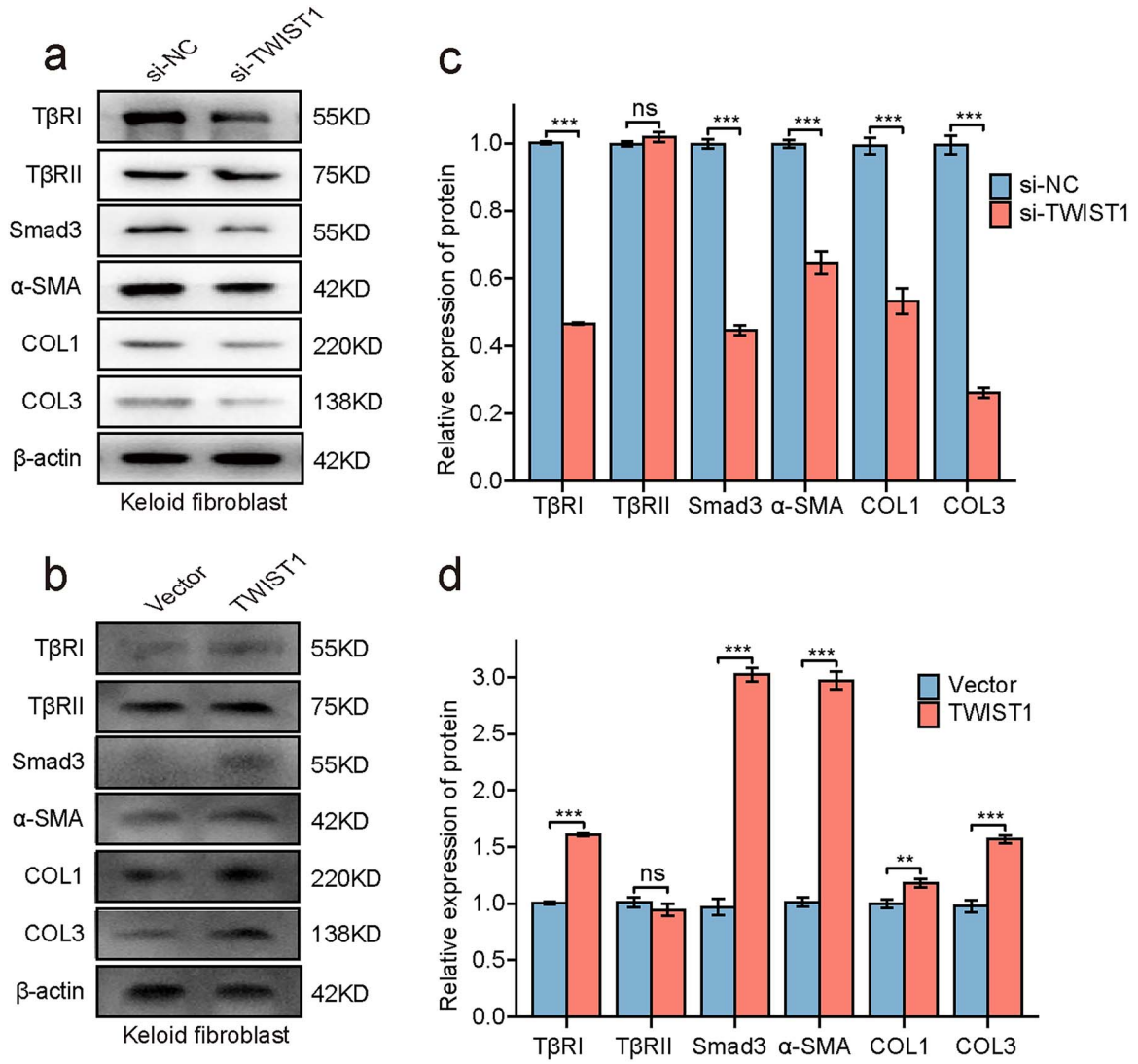

Figure 3. TWIST1 knockdown and overexpression affect the expression of the TGFβ/Smad signaling-related molecules TBR1, Smad2 and Smad3, and the fibrosis markers α-SMA, COL1 and COL3. (**a**) Protein expression of TβRI, TβRII and Smad3, and fibrosis markers α-SMA, COL1 and COL3 in small interfering negative control and small interfering TWIST1 groups was detected by western blotting. (**b**) Protein expression of TβRI, TβRII and Smad3 and the fibrosis markers α-SMA, COL1 and COL3 in vector and TWIST1 groups was detected by western blotting. (**c**, **d**) Densitometry analysis of western blot results. $^{**}p < 0.01$, $^{***}p < 0.001$; ns not significant. *TβR1* transforming growth factor beta receptor 1, *SMAD3* SMAD family member 3, *COL1* collagen type I, *COL3* collagen type III, *NC* negative control

expression levels in comparison to the vector groups (Figure S2c, d, see online supplementary material). The assays that followed employed cells that were stably infected. We further confirmed the capacity of TWIST1 to affect the biological behavior of KFBs. The CCK-8 assay showed that downregulating TWIST1 significantly reduced the capacity of KFBs to proliferate ($p < 0.05$). In contrast, overexpression of TWIST1 significantly improved KFBs' capacity for proliferation (Figure 2a, b; $p < 0.05$). Transwell assays showed that overexpression of TWIST1 greatly increased the invasion ability of KFBs, and knockdown of TWIST1 significantly decreased the invasion ability (Figure 2c, d; $p < 0.05$). Furthermore, we validated the effect of TWIST1 on downstream factors of the EMT pathway in KFBs. Using RT–PCR, we revealed that knockdown of TWIST1 dramatically decreased the mRNA expression of E-cadherin and increased the expression of N-cadherin, vimentin and fibronectin and vice versa (Figure S2e, f, see online supplementary material). Additionally, immunofluorescence labeling showed that si-TWIST1 dramatically reduced the production of α-SMA that was induced by TGF-β1, indicating the significance of TWIST1's role in fibroblast activation (Figure 2e). In addition, we also interfered with NFBs using siRNAs and overexpression plasmids (Figure S3a, b, see online supplementary material). Using CCK-8 and transwell experiments, we found that the effect of TWIST1 on the proliferation and invasion ability of NFBs was not significant (Figure S3c–f, see online supplementary material).

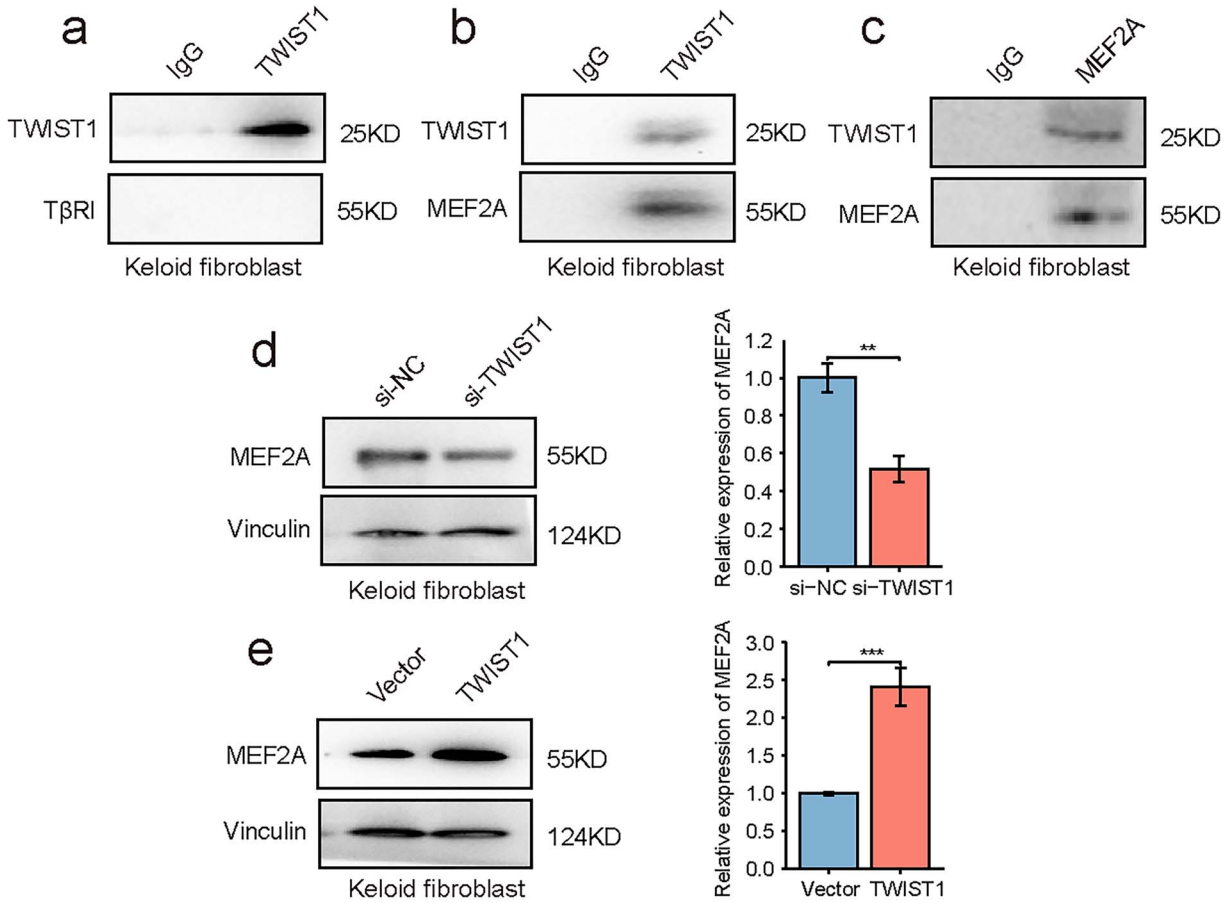

Figure 4. TWIST1 interacts with MEF2A and regulates MEF2A expression. (**a**, **b**) Cell lysates of keloid-derived fibroblasts were immunoprecipitated with anti-TWIST1 antibody, followed by immunoblotting with anti-TβRI or anti-MEF2A antibody, respectively. (**c**) Cell lysates of keloid-derived fibroblasts were immunoprecipitated with anti-MEF2A antibody, followed by immunoblotting with anti-TWIST1 and anti-MEF2A antibody; IgG was used as a negative control. (**d**) Protein expression of MEF2A in small interfering negative control and small interfering TWIST1 groups was detected by western blotting with densitometry analysis of western blot results. (**e**). Protein expression of MEF2A in vector and TWIST1 groups was detected by western blotting with densitometry analysis of western blot results. $^{**}p < 0.01$, $^{***}p < 0.001$. *IgG* immunoglobulin G, *TWIST1* Twist-related protein 1, *MEF2A* myocyte enhancer factor 2A, *NC* negative control

TWIST1 enhances the expression of TBR1, Smad3, α-SMA, collagen type I and collagen type III We further investigated TWIST1's ability to affect TGF-β/Smad signaling. Using RT–PCR, we revealed that knockdown of TWIST1 dramatically decreased the mRNA expression of TGF-β/Smad signaling components, including TBR1, Smad3, α-SMA, collagen type I (COL1) and collagen type III (COL3) (Figure S4a, see online supplementary material). On the other hand, TWIST1 overexpression also markedly elevated the mRNA expression of TBR1, Smad3, α-SMA, COL1 and COL3 (Figure S4b, see online supplementary material). We showed that knockdown of TWIST1 dramatically reduced the expression levels of TGF-β/Smad signaling proteins, including TBR1, Smad3, α-SMA, COL1 and COL3, using Western blot analysis (Figure 3a, b). On the other hand, TWIST1 overexpression also markedly increased the levels of TBR1, Smad3, α-SMA, COL1 and COL3 protein expression (Figure 3c, d). Combined, these findings suggested that TWIST1 could improve TGF-β/Smad signaling.

TWIST1 interacts with MEF2A in KFBs

Since enhanced KFB activation, proliferation and invasion has been mechanistically linked to increased TBR1 expression, we next investigated whether the negative effects of TWIST1 in keloids may be connected to altered TBR1 gene expression [26,27]. By attaching to E-box elements, TWIST1 controls the expression of the target gene. Although we hypothesized that TWIST1 might directly interact with the TBR1 promoter region, the coimmunoprecipitation results showed no evidence of this (Figure 4a). Additionally, a bioinformatic search revealed no direct relationship between TWIST1 and the TBR1 promoter (http://cistrome.org/db/#/). Hence, we hypothesized that TWIST1 might control gene expression through a molecular partner.

A total of 508 proteins were discovered by mass spectrometry analysis to probably interact with TWIST1. Our focus was on MEF2A, a significant transcription factor linked to fibroblast development [28]. MEF2A was pulled down by TWIST1 immunoprecipitation and vice versa in human KFBs,

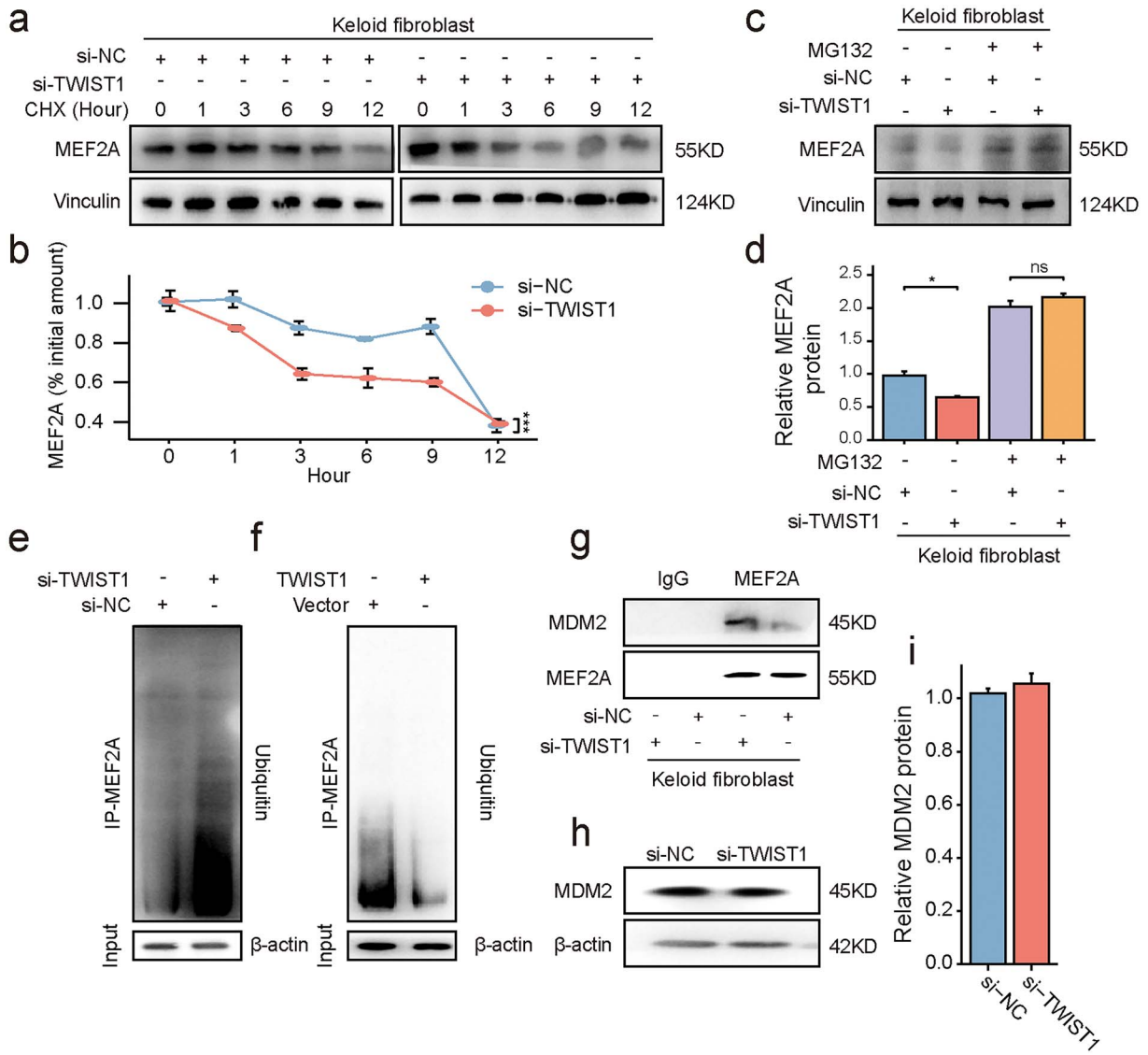

Figure 5. TWIST1 suppress ubiquitination and degradation of MEF2A. (**a**) Western blotting detected the alteration of MEF2A in small interfering negative control and small interfering TWIST1 groups treated with 10 μg/ml cycloheximide (CHX) for the indicated times. (**b**) Densitometric analysis of MEF2A from experiments. (**c**) Keloid-derived fibroblasts transfected by si-NC or si-TWIST1 were treated with 10 nmol/ml MG132, and protein concentrations of MEF2A were determined. (**d**) Densitometric analysis of MEF2A from experiments. (**e, f**) Lysates from keloid-derived fibroblasts modulated with down- or up-regulated TWIST1 were incubated with anti-MEF2A antibody. Immunoprecipitants were immunoblotted with an anti-Ub (ubiquitin) antibody. (**g**) Coimmunoprecipitation of MDM2 and MEF2A in keloid-derived fibroblasts transfected with si-NC or si-TWIST1. (**h, i**) Protein concentrations of MDM2 in keloid-derived fibroblasts transfected with si-NC or si-TWIST1. $^*P < 0.05$, $^{***}p < 0.001$; ns not significant. *Ub* ubiquitin, *TWIST1* Twist-related protein 1, *MEF2A* myocyte enhancer factor 2A, *NC* negative control, *CHX* cycloheximide, *MDM2* mouse double minute 2 homolog, *si* small interfering

demonstrating a direct relationship between the two proteins (Figure 4b, c).

The next step was to determine whether MEF2A works as a downstream target of TWIST1 in KFBs. TWIST1 silencing significantly decreased MEF2A concentrations, whereas TWIST1 overexpression in KFBs increased MEF2A concentrations (Figure 4d, e). TWIST1 knockdown or overexpression, however, had no effect on MEF2A mRNA levels in KFBs, showing that TWIST1 directly regulates MEF2A protein concentrations, most likely by inhibiting its degradation (Figure S5a, b, see online supplementary material).

TWIST1 inhibits the ubiquitination and proteasomal degradation of MEF2A. Using cycloheximide chase experiments, we demonstrated that TWIST1 overexpression enhanced the half-life of MEF2A in KFBs (Figure 5a, b). These results led us to investigate whether TWIST1 might increase MEF2A degradation by the ubiquitin proteasome pathway. After TWIST1 knockdown, the loss of MEF2A was prevented by the proteasome inhibitor MG132, indicating that TWIST1 specifically targets MEF2A and suppresses its proteasomal degradation (Figure 5c, d). TWIST1 consistently regulated the level of ubiquitination of MEF2A in KFBs

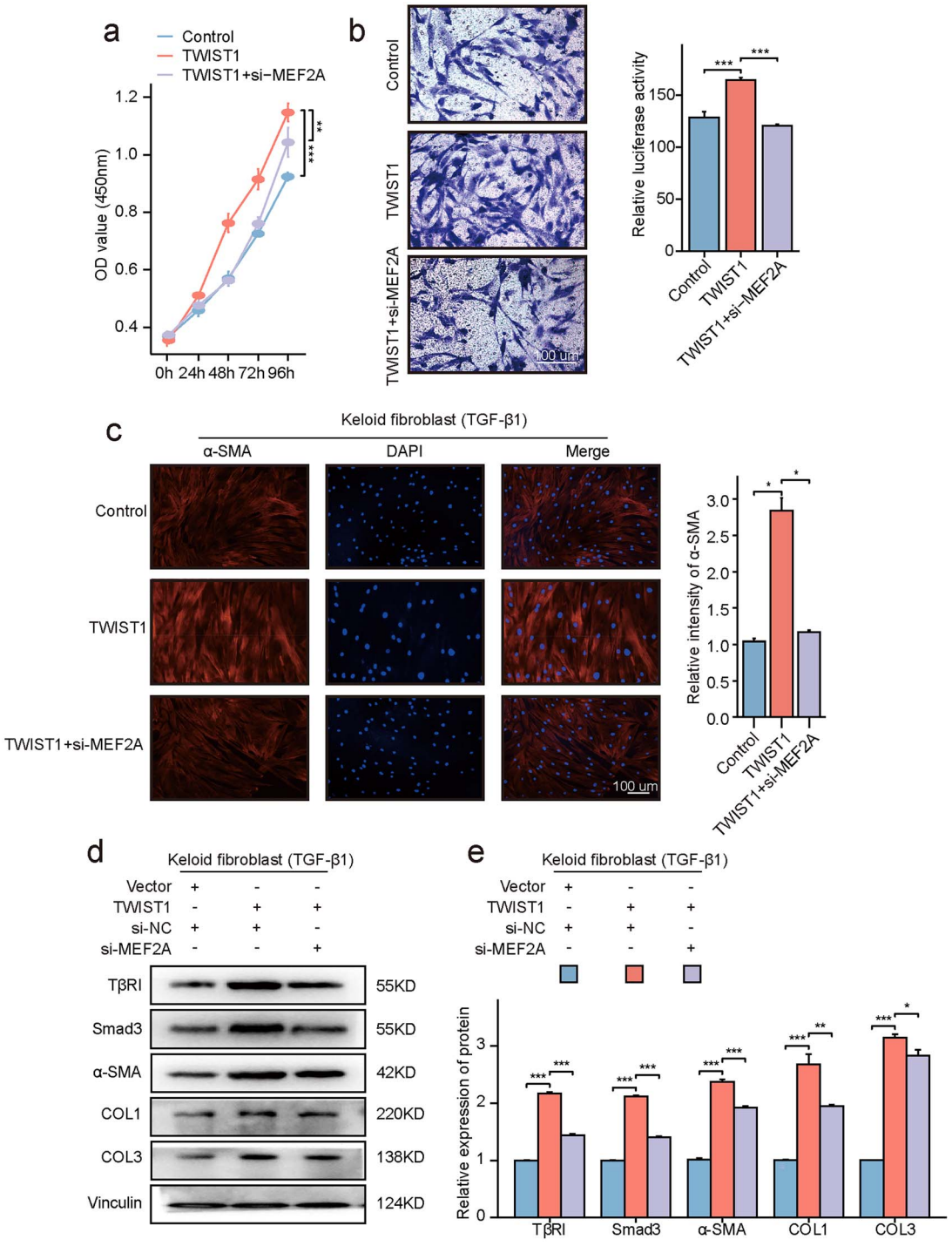

Figure 6. TWIST1 promoted a profibrotic phenotype via the MEF2A-dependent TGF-β pathway in keloid derived fibroblasts. (**a**) Proliferation ability of keloid-derived fibroblasts transfected by control or TWIST1 or TWIST1 with si-MEF2A was measured using a growth curve. (**b**) Cell invasion determined by transwell in pretreated keloid-derived fibroblasts (Scale bar: 100 μm). (**c**) Keloid-derived fibroblasts transfected by control or TWIST1 or TWIST1 with si-MEF2A pretreated with 5 ng/ml TGF-β1 were measured by α-SMA using an immunofluorescence assay (Scale bar: 100 μm). (**d**, **e**) Protein levels of TβRI, Smad3 and α-SMA were detected by Western blotting. Vinculin was used as internal control. $^{*}p < 0.05$, $^{**}p < 0.01$, $^{***}p < 0.001$. *TWIST1* Twist-related protein 1, *MEF2A* myocyte enhancer factor 2A, *NC* negative control, *TβR1* transforming growth factor beta receptor 1, *SMAD3* SMAD family member 3, *COL1* collagen type I, *COL3* collagen type III

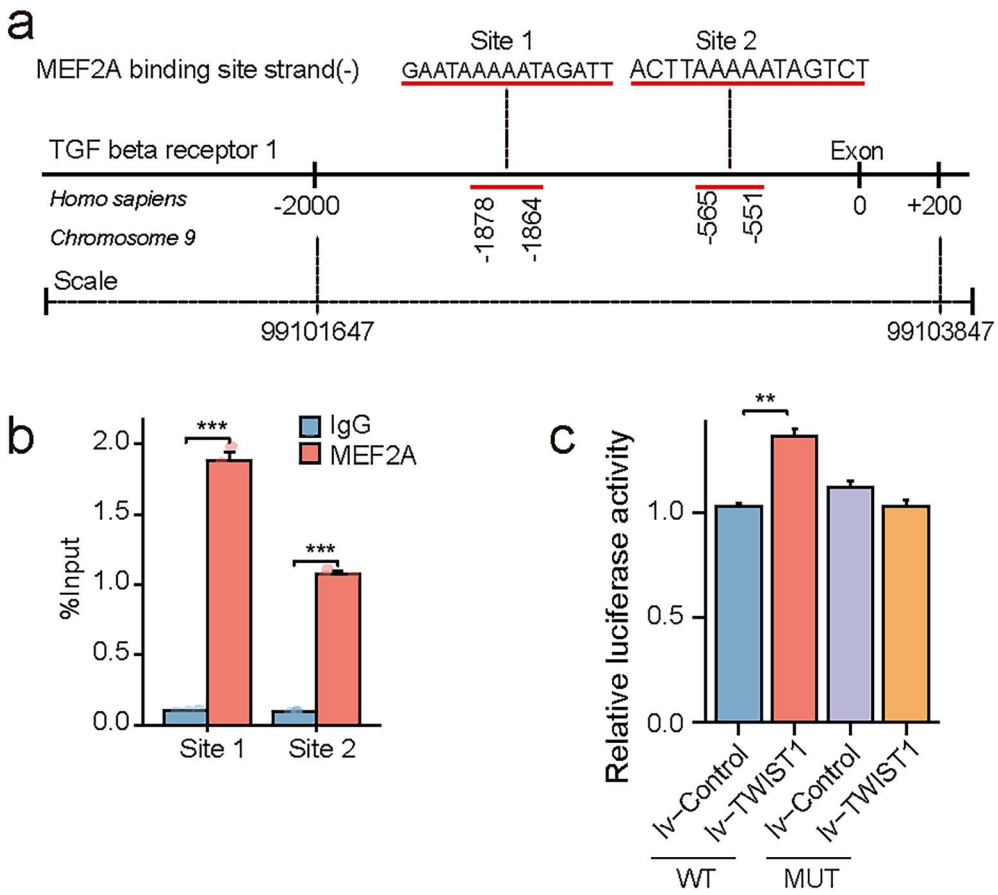

Figure 7. TGF-β receptor 1 (TBR1) was a direct target of MEF2A in keloid-derived fibroblasts. (**a**) Prediction of MEF2A-binding sites in the TBR1 promoter region using JASPAR software. (**b**) ChIP-qPCR assay showed the binding capability of MEF2A with different predicted binding sites. (**c**) Dual-luciferase reporter assay indicated the promoter activity of MEF2A encoding wild-type (WT) or mutant (MUT) MEF2A-binding site. $^{**}p < 0.01$, $^{***}p < 0.001$. *WT* wild-type, *MUT* mutant, MEF2A myocyte enhancer factor 2A, *IgG* immunoglobulin G

(Figure 5e, f). Co-immunoprecipitation assays revealed a connection between MEF2A and mouse double minute 2 homolog (MDM2), the E3 ubiquitin-protein ligase for MEF2A, which was diminished by TWIST1 silencing (Figure 5g). Interestingly, this effect was not attributed to a reduction in total MDM2 expression, as si-TWIST1 had no influence on this (Figure 5h, i). Our results suggest that TWIST1 suppresses MDM2-mediated ubiquitination and MEF2A proteasomal degradation.

TWIST1 stimulates KFB proliferation via MEF2A

Next, we evaluated the functional relevance of MEF2A for TWIST1-dependent KFB behaviors. Using western blotting and immunohistochemistry, we demonstrated that MEF2A was expressed at a higher level in keloid tissues than in normal skin tissues (Figure S5c-e, see online supplementary material). Additionally, by extracting fibroblasts, we found that MEF2A expression was higher in KFBs than in NFBs (Figure S5f, see online supplementary material). The expression of TBR1, Smad3 and α-SMA in KFBs was decreased by MEF2A knockdown (Figure S5g-i, see online supplementary material).

Further investigating this hypothesis, we examined whether the biological behavior of TWIST1-overexpressing KFBs could be rescued by inhibiting MEF2A. Accordingly, MEF2A knockdown significantly attenuated the effect of TWIST1 overexpression on KFB proliferation, invasion and fibroblast activation (Figures 6a–c). Similarly, after TWIST1 overexpression, MEF2A knockdown restored TBR1, Smad3, α-SMA, COL1 and COL3 expression (Figure 6d, e). Our findings identify MEF2A as a downstream regulator of TWIST1-dependent KFB proliferation, invasion and fibroblast activation.

TBR1 was the direct target of MEF2A in KFBs

Chip-qPCR analysis was performed using primers created in accordance with the JASPAR database's predicted binding site for MEF2A (Table S5, see online supplementary material) on the TBR1 promoter. The findings demonstrated that MEF2A had a better ability to attach to DNA sequences from the TBR1 region −1878 to −1864 than to another binding site (−565 to −551) (Figure 7a, b). Moreover, a dual-luciferase reporter gene was constructed to identify

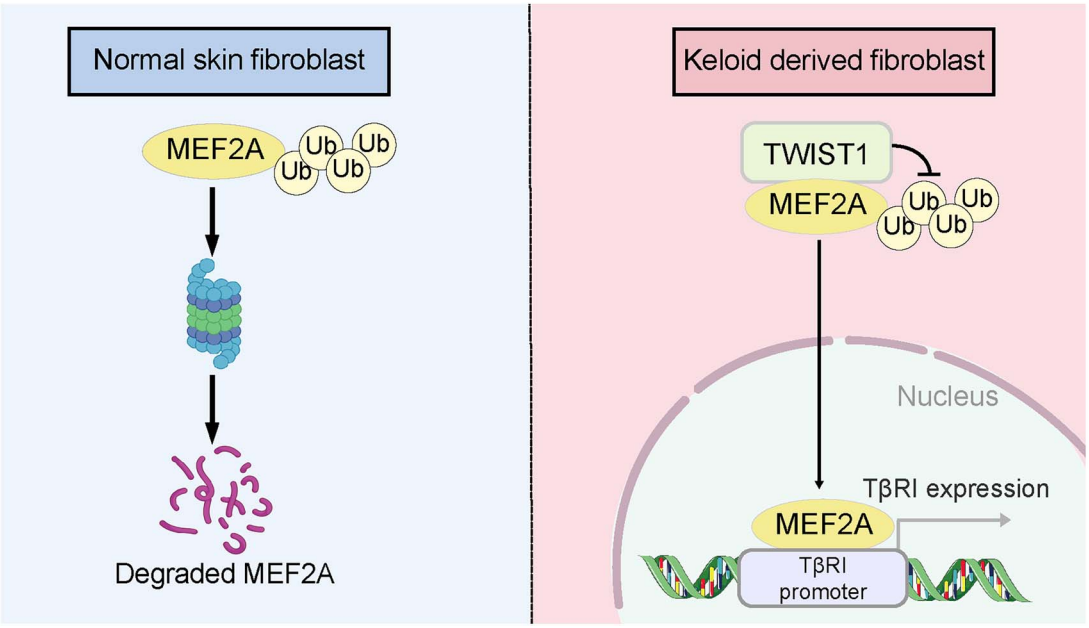

Figure 8. Schematic representation of TWIST1 promoting expression of TGF-β receptor 1 by regulating the stability of MEF2A. *TWIST1* Twist-related protein 1, *MEF2A* myocyte enhancer factor 2A, *TβR1* transforming growth factor beta receptor 1, *Ub* ubiquitin

MEF2A promoter activity. The outcomes demonstrated that relative luciferase activity was increased in the wild-type-promoter group following MEF2A elevation but remained unaltered in the mutated-promoter group (Figure 7c). According to these findings, MEF2A is directly linked to the TBR1 promoter at the designated DNA regions, activating the transcription of TBR1 (Figure 8).

Discussion

In this article, we report a unique role for TWIST1 as a promoter of KFB proliferation, invasion and fibroblast activation. We also present a novel mechanism for TWIST1 in KFBs, in which TWIST1 increases TBR1 through suppressed degradation of the transcription factor MEF2A, which directly interacts with the TBR1 promoter and controls TBR1 transcription. Thus, TWIST1 inhibition may offer an effective way to prevent keloids.

The healing process of skin wounds involves a complex coordination and interaction between the processes of re-epithelialization and granulation formation. A poorly healed skin wound can easily contribute to the formation of scars, including hyperplastic scars and keloids. Research has shown specimens from patients with hyperplastic scars with a significant thickening of the epidermis of the scars and basement membrane degradation [29]. Further analysis revealed that TWIST1 expression was also significantly increased in scar tissue and that EMT in scar tissue was associated with elevated levels of local inflammatory factors [29]. Meanwhile, studies have shown that EMT may occur in tissues such as epidermis, hair follicles and microvasculature of keloids, accompanied by high expression of EMT molecules such as TWIST1 [30].

TWIST1 was originally discovered to be a developmental process regulator in Drosophila embryos [31]. TWIST1 regulates a number of physiologic and pathological processes in vertebrates [14,32,33]. We observed increased TWIST1 expression not only following TGF-β1 stimulation *in vitro* but also in keloid tissue when compared with normal skin tissue. Silencing TWIST1 reduced KFB activation, invasion and proliferation. The TBR1 gene in KFBs was positively modulated by TWIST1 during transcription. Although TWIST1 is known to function as a transcriptional modulator that can perform with a certain E-box motif, a search of the chromatin immunoprecipitation sequence database did not find any evidence of a direct relationship between TWIST1 and the TBR1 promoter. However, we discovered a unique molecular relationship between TWIST1 and MEF2A in which TWIST1 promoted MEF2A binding to MDM2 to increase MEF2A expression. However, TWIST1 had no effect on the levels of MDM2 proteins, indicating that the interaction between TWIST1 and MEF2A may have changed the way the MEF2A protein conforms, making it easier for it to connect to MDM2. However, this hypothesis is yet to be verified.

The MEF2 proteins are transcriptional regulators from the Minichromosome Maintenance 1 (MCM)-1-agamous-deficiens serum response factor family [34,35]. Previous research has shown that MEF2 is essential for numerous physiological and pathological processes [36,37]. MEF2A, the most prevalent family member expressed in fibroblasts and previously associated with hypertrophic scarring but not keloids, is one of the known MEF2 proteins [38,39]. In this article, we demonstrate that KFBs and keloid tissue both exhibit a significant upregulation of MEF2A. The unique keloid remodeling mechanism we present further identifies

MEF2A as a molecular partner of TWIST1 with biological consequences in KFBs. TWIST1 enhances MEF2A expression through reduced MDM2-mediated protein degradation.

TBR1 is the most prominent gene associated with fibrosis, and acquired expression of the TBR1 gene is a common trait in patients with keloids [40–42]. Increasing evidence suggests that functional TBR1 gain has a causal role in the dysregulated proliferation of KFBs. Here, we found that MEF2A is a novel transcription factor that binds to the promoter region of the TBR1 gene and directly controls the gene's expression. This finding offers a potential mechanistic explanation for how TWIST1 promotes TBR1 transcription. The study demonstrated that TWIST1 promotes KFB proliferation and invasion by increasing the quantity of MEF2A and probably by restoring TBR1 expression, supporting this mechanistic connection. On the other hand, TWIST downregulation increased proteasomal MEF2A degradation and hence decreased the amount of MEF2A at the TBR1 promoter.

However, it is crucial to keep in mind that, just as transcription factors other than MEF2A and epigenetic processes may be involved in the rise of TBR1 in keloids, the regulation of MEF2A and TBR1 may just represent one of numerous paths for the proliferative effects of TWIST1. Our study's focus on TWIST1's impact on keloid KFBs specifically poses additional limitations. TWIST1, in addition to the above roles in KFBs, has been reported to be associated with severe inflammatory [43–45]. Future investigations into the promotion of the fibrosis effect of TWIST1 in hypertrophic scar and keloid development are needed in light of the growing significance of fibrosis in scar formation. The lack of cell-type specificity and potential off-target effects of TWIST1 inhibition by harmine should also be taken into consideration, as well as the typically limited capacity of preventive therapies to translate from the keloid model to the clinical setting.

Overall, we demonstrated the critical function of TWIST1 in keloids. More specifically, we showed that the connection between TWIST1 and MEF2A, in which TWIST1 promotes MEF2A-mediated TBR1 transcription and induces activation of the TGF-β/Smad pathway, is what causes fibroblast activation. TWIST1 shows potential for the treatment of keloid and other fibroproliferative diseases.

Conclusions

Our research identifies a pivotal role of TWIST1 in keloid pathogenesis, particularly in fibroblasts, which is partly mediated by elevated MEF2A-dependent TBR1 expression. Blocking TWIST1 activity in keloid fibroblasts may represent a novel therapeutic approach for treating keloid disease. Our findings enhance understanding of keloid pathogenesis and suggest new directions for targeted therapies. Future studies could explore specific inhibitors of TWIST1 and test their efficacy in preclinical models.

Abbreviations

COL1: Collagen I; COL3: Collagen III; EMT: Epithelial-to-mesenchymal transition; KFB: Keloid-derived fibroblasts; NFB: Normal skin-derived fibroblasts; MEF2A: Myocyte enhancer factor 2A; TBST: Tris-buffered saline with 0.05% Tween.

Supplementary data

Supplementary data is available at *Burns & Trauma Journal* online.

Funding

This study was funded by the National High Level Hospital Clinical Research Funding, grant No. 2022-PUMCH-C-041, the Medical Science and Health Technology Innovation Project (2022-I2M-1-068), the Medical Science and Health Technology Innovation Project (2021-I2M-1-003) and Young Scientists Fund of the Natural Science Foundation of Sichuan (2024NSFSC1505).

Authors' contributions

TL performed experiments, data analyses and wrote the original manuscript. MZ, YL, YS, JH and AZ performed data analyses, wrote and critically reviewed the manuscript. NY and XL conceived, designed and directed the study.

Ethics approval and consent to participate

This study which involved human participants was examined and approved by the Peking Union Medical College. Patients/participants provided written informed consent to participate in this research.

Conflict of interest

None declared.

References

1. Tsai CH, Ogawa R. Keloid research: current status and future directions. *Scars, burns & healing*. 2019;5:205951311986865.
2. Naik PP. Novel targets and therapies for keloid. *Clin Exp Dermatol*. 2022;47:507–15.
3. Ogawa R. Keloid and hypertrophic scars are the result of chronic inflammation in the reticular dermis. *Int J Mol Sci*. 2017;18:606
4. Direder M, Weiss T, Copic D, Vorstandlechner V, Laggner M, Pfisterer K, *et al*. Schwann cells contribute to keloid formation. *Matrix biology : journal of the International Society for Matrix Biology*. 2022;108:55–76.
5. Lee HJ, Jang YJ. Recent understandings of biology, prophylaxis and treatment strategies for hypertrophic scars and keloids. *Int J Mol Sci*. 2018;19:711
6. Ogawa R. The most current algorithms for the treatment and prevention of hypertrophic scars and keloids: a 2020 update of the algorithms published 10 years ago. *Plast Reconstr Surg*. 2022;149:79e–4.
7. Xia Y, Wang Y, Shan M, Hao Y, Liang Z. Decoding the molecular landscape of keloids: new insights from single-cell transcriptomics. *Burns & Trauma*. 2023;11:tkad017.
8. Ud-Din S, Bayat A. Keloid scarring or disease: unresolved quasi-neoplastic tendencies in the human skin. *Wound repair and regeneration : official publication of the Wound Healing Society [and] the European Tissue Repair Society*. 2020;28:422–6.

9. Walsh LA, Wu E, Pontes D, Kwan KR, Poondru S, Miller CH, *et al.* Keloid treatments: an evidence-based systematic review of recent advances. *Systematic reviews*. 2023;12:42.
10. Liu X, Chen W, Zeng Q, Ma B, Li Z, Meng T, *et al.* Single-cell RNA-sequencing reveals lineage-specific regulatory changes of fibroblasts and vascular endothelial cells in keloids. *The Journal of investigative dermatology*. 2022;142:124–135.e111.
11. Shim J, Oh SJ, Yeo E, Park JH, Bae JH, Kim SH, *et al.* Integrated analysis of single-cell and spatial Transcriptomics in keloids: highlights on Fibrovascular interactions in keloid pathogenesis. *The Journal of investigative dermatology*. 2022;142:2128–2139.e2111.
12. Dai S, Xu M, Pang Q, Sun J, Lin X, Chu X, *et al.* Hypoxia macrophage-derived exosomal miR-26b-5p targeting PTEN promotes the development of keloids. *Burns & Trauma*. 2024;12:tkad036.
13. Wang YZ, Su C, Fu SQ, Liu LQ. Research advances on the characteristics of fibroblast in keloid. *Zhonghua shao shang yu chuang mian xiu fu za zhi*. 2022;38:590–4.
14. Yang J, Mani SA, Donaher JL, Ramaswamy S, Itzykson RA, Come C, *et al.* Twist, a master regulator of morphogenesis, plays an essential role in tumor metastasis. *Cell*. 2004;117:927–39.
15. Murre C, McCaw PS, Vaessin H, Caudy M, Jan LY, Jan YN, *et al.* Interactions between heterologous helix-loop-helix proteins generate complexes that bind specifically to a common DNA sequence. *Cell*. 1989;58:537–44.
16. Gort EH, van Haaften G, Verlaan I, Groot AJ, Plasterk RH, Shvarts A, *et al.* The TWIST1 oncogene is a direct target of hypoxia-inducible factor-2alpha. *Oncogene*. 2008;27:1501–10.
17. Yoo YG, Christensen J, Gu J, Huang LE. HIF-1α mediates tumor hypoxia to confer a perpetual mesenchymal phenotype for malignant progression. *Sci Signal*. 2011;4:pt4.
18. Kang Y, Massagué J. Epithelial-mesenchymal transitions: twist in development and metastasis. *Cell*. 2004;118:277–9.
19. Pozharskaya V, Torres-González E, Rojas M, Gal A, Amin M, Dollard S, *et al.* Twist: a regulator of epithelial-mesenchymal transition in lung fibrosis. *PLoS One*. 2009;4:e7559.
20. Ning X, Zhang K, Wu Q, Liu M, Sun S. Emerging role of Twist1 in fibrotic diseases. *J Cell Mol Med*. 2018;22:1383–91.
21. Palumbo-Zerr K, Soare A, Zerr P, Liebl A, Mancuso R, Tomcik M, *et al.* Composition of TWIST1 dimers regulates fibroblast activation and tissue fibrosis. *Ann Rheum Dis*. 2017;76:244–51.
22. Pardali E, ten Dijke P. Transforming growth factor-beta signaling and tumor angiogenesis. *Frontiers in bioscience (Landmark edition)*. 2009;14:4848–61.
23. Macarak EJ, Wermuth PJ, Rosenbloom J, Uitto J. Keloid disorder: fibroblast differentiation and gene expression profile in fibrotic skin diseases. *Exp Dermatol*. 2021;30:132–45.
24. Piersma B, Bank RA, Boersema M. Signaling in fibrosis: TGF-β, WNT, and YAP/TAZ converge. *Front Med*. 2015;2:59.
25. Li T, Huang J, Zeng A, Yu N, Long X. Ubiquitin-specific peptidase 11 promotes development of keloid derived fibroblasts by de-ubiquitinating TGF-β receptorII. *Burns. journal of the International Society for Burn Injuries*. 2023;50(3):641–652.
26. Gao S, Li X, Jiang Q, Liang Q, Zhang F, Li S, *et al.* PKM2 promotes pulmonary fibrosis by stabilizing TGF-β1 receptor I and enhancing TGF-β1 signaling. *Sci Adv*. 2022;8:eabo0987.
27. Song MK, Lee JH, Ryoo IG, Lee SH, Ku SK, Kwak MK. Bardoxolone ameliorates TGF-β1-associated renal fibrosis through Nrf2/Smad7 elevation. *Free Radic Biol Med*. 2019;138:33–42.
28. Gao Y, Liu Y, Zheng D, Ho C, Wen D, Sun J, *et al.* HDAC5-mediated Smad7 silencing through MEF2A is critical for fibroblast activation and hypertrophic scar formation. *Int J Biol Sci*. 2022;18:5724–39.
29. Yan C, Grimm WA, Garner WL, Qin L, Travis T, Tan N, *et al.* Epithelial to mesenchymal transition in human skin wound healing is induced by tumor necrosis factor-alpha through bone morphogenic protein-2. *Am J Pathol*. 2010;176:2247–58.
30. Yan L, Cao R, Wang L, Liu Y, Pan B, Yin Y, *et al.* Epithelial-mesenchymal transition in keloid tissues and TGF-β1-induced hair follicle outer root sheath keratinocytes. *Wound repair and regeneration : official publication of the Wound Healing Society [and] the European Tissue Repair Society*. 2015;23:601–10.
31. Fan Y, Gu X, Zhang J, Sinn K, Klepetko W, Wu N, *et al.* TWIST1 drives smooth muscle cell proliferation in pulmonary hypertension via loss of GATA-6 and BMPR2. *Am J Respir Crit Care Med*. 2020;202:1283–96.
32. Howard TD, Paznekas WA, Green ED, Chiang LC, Ma N. Ortiz de Luna RI, Garcia Delgado C, Gonzalez-Ramos M, Kline AD, jabs EW: mutations in TWIST, a basic helix-loop-helix transcription factor. *Saethre-Chotzen syndrome Nature genetics*. 1997;15:36–41.
33. Lovisa S, LeBleu VS, Tampe B, Sugimoto H, Vadnagara K, Carstens JL, *et al.* Epithelial-to-mesenchymal transition induces cell cycle arrest and parenchymal damage in renal fibrosis. *Nat Med*. 2015;21:998–1009.
34. Di Giorgio E, Hancock WW, Brancolini C. MEF2 and the tumorigenic process, hic sunt Leones. *Biochimica et biophysica acta Reviews on cancer*. 2018;1870:261–73.
35. Dietrich JB. The MEF2 family and the brain: from molecules to memory. *Cell Tissue Res*. 2013;352:179–90.
36. Chen X, Gao B, Ponnusamy M, Lin Z, Liu J. MEF2 signaling and human diseases. *Oncotarget*. 2017;8:112152–65.
37. Cornwell JD, McDermott JC. MEF2 in cardiac hypertrophy in response to hypertension. *Trends in cardiovascular medicine*. 2022;33(4):204–212.
38. Pon JR, Marra MA. MEF2 transcription factors: developmental regulators and emerging cancer genes. *Oncotarget*. 2016;7:2297–312.
39. Taylor MV, Hughes SM. Mef2 and the skeletal muscle differentiation program. *Semin Cell Dev Biol*. 2017;72:33–44.
40. Bran GM, Goessler UR, Schardt C, Hormann K, Riedel F, Sadick H. Effect of the abrogation of TGF-beta1 by antisense oligonucleotides on the expression of TGF-beta-isoforms and their receptors I and II in isolated fibroblasts from keloid scars. *Int J Mol Med*. 2010;25:915–21.
41. Chu Y, Guo F, Li Y, Li X, Zhou T, Guo Y. A novel truncated TGF-beta receptor II downregulates collagen synthesis and TGF-beta I secretion of keloid fibroblasts. *Connect Tissue Res*. 2008;49:92–8.
42. Lei R, Li J, Liu F, Li W, Zhang S, Wang Y, *et al.* HIF-1α promotes the keloid development through the activation of TGF-β/Smad and TLR4/MyD88/NF-κB pathways. *Cell cycle (Georgetown, Tex)*. 2019;18:3239–50.

43. Ding X, Li F, Zhang L. Knockdown of Delta-like 3 restricts lipopolysaccharide-induced inflammation, migration and invasion of A2058 melanoma cells via blocking Twist1-mediated epithelial-mesenchymal transition. *Life Sci*. 2019;226:149–55.
44. Li A, Zhao F, Yang T, Zhao Y, Liu H, Yang S, *et al*. PTX3/TWIST1 feedback loop modulates lipopolysaccharide-induced inflammation via PI3K/Akt Signaling pathway. *Journal of interferon & cytokine research : the official journal of the International Society for Interferon and Cytokine Research*. 2022;42:161–9.
45. Zhao X, Deng R, Wang Y, Zhang H, Dou J, Li L, *et al*. Twist1/Dnmt3a and miR186 establish a regulatory circuit that controls inflammation-associated prostate cancer progression. *Oncogenesis*. 2017;6:e315.